Received: 22 November 2021 | Revised: 17 March 2022 | Accepted: 18 March 2022

DOI: 10.1111/mpp.13217

Molecular Plant Pathology WILEY

ORIGINAL ARTICLE

CsrD regulates amylovoran biosynthesis and virulence in *Erwinia amylovora* in a novel cyclic-di-GMP dependent manner

Roshni R. Kharadi | **George W. Sundin**

Department of Plant, Soil and Microbial Sciences, Michigan State University, East Lansing, Michigan, USA

Correspondence
George W. Sundin, Department of Plant, Soil and Microbial Sciences, Michigan State University, East Lansing, MI, USA.
Email: sundin@msu.edu

Funding information
National Institute of Food and Agriculture, Grant/Award Number: 2015-67013-23068

Abstract

Erwinia amylovora is an economically devastating plant pathogen that causes fire blight disease in members of the Rosaceae family, most notably in apple and pear. The exopolysaccharide amylovoran is a pathogenicity determinant in *E. amylovora* and a major component of the extracellular matrix of biofilms formed within the xylem vasculature of the host plant. The second messenger cyclic-di-GMP (c-di-GMP) has been reported to positively regulate the transcription of *amsG* (the first gene in the 12-gene amylovoran [*ams*] biosynthetic operon), thus impacting amylovoran production. However, the regulatory mechanism by which this interaction occurs is largely unknown. Here, we report that c-di-GMP can bind to specific residues in the EAL domain of the *E. amylovora* protein CsrD. CsrD and RNase E regulate the degradation of the sRNA CsrB in *E. amylovora*. When CsrD is bound to c-di-GMP, there is an enhancement in the level of RNase E-mediated degradation of CsrB, which then alters *amsG* transcription. Additionally, *csrD* was also found to positively contribute to virulence and biofilm formation. We thus present a pathway of conditional regulation of amylovoran production mediated by changing intracellular levels of c-di-GMP, which impacts disease progression.

KEYWORDS
CsrA, CsrB, cyclic-di-GMP, exopolysaccharide, fire blight, RNase E, smallRNA

1 | INTRODUCTION

The bacterial second messenger molecule bis-(3′,5′)-cyclic diguanosine monophosphate (c-di-GMP) is a key regulator of the bidirectional transition between a motile and a sessile lifestyle (Jenal et al., 2017). Diguanylate cyclases (Dgc enzymes), marked by the presence of a GGDEF domain, dimerize GTP molecules to form c-di-GMP, and phosphodiesterases (Pde enzymes), characterized by the presence of an EAL or HD-GYP domain, hydrolyse c-di-GMP into 5′-phosphoguanylyl-(3′,5′)-guanosine (pGpG) or GMP, respectively (Jenal et al., 2017).

c-di-GMP signalling has been shown to regulate several virulence factors at different levels in various plant-pathogenic bacteria. In *Dickeya dadantii* 3937, multiple c-di-GMP effectors including two Pdes, EcpC and EGcpB, regulate the type III secretion system through *hrpA* expression at a transcriptional level (Yuan et al., 2015). Similarly, in *Pseudomonas syringae* pv. *tomato* DC3000, the Dgc protein PleD can negatively regulate *hrpL* and *hrpA* transcription (Perez-Mendoza et al., 2014). In *Xanthomonas oryzae* PX099 and in *Xylella fastidiosa* Temecula, the negative regulation of extracellular polysaccharide (EPS) formation and flagellar motility are channelled through specific Dgc enzymes as well (Chatterjee et al., 2010; Yang

et al., 2016) The regulatory effect of c-di-GMP in plant-pathogenic bacteria is predominantly understood through the phenotypic effect resulting from the loss of a *dgc* or *pde* gene and the subsequent changes in intracellular c-di-GMP levels.

CsrA (carbon storage regulator A) (alternatively annotated as RsmA; regulator of secondary metabolism) is a global bacterial regulator that can modulate genes at a transcriptional or a posttranscriptional level (Kusmierek & Dersch, 2018). CsrA activity and availability are regulated by the small RNAs (sRNAs) CsrB and CsrC though binding and functional sequestration of CsrA (Liu et al., 1997; Suzuki et al., 2002). Additionally, in *Escherichia coli* K-12, CsrD is an RNase E specificity factor that can enhance the degradative activity of RNase E towards the sRNAs CsrB and CsrC (Suzuki et al., 2006). A proteomic approach used to identify the regulatory network of CsrA in *Xanthomonas citri* Xcc306 revealed that this network includes several proteins involved in flagellar biosynthesis and chemotaxis as well as type II and type IV secretion (Andrade et al., 2021). In *P. syringae* DC3000, CsrA was found to be a global regulator of virulence, EPS synthesis, motility, and growth (Ferreiro et al., 2018). In *Xanthomonas campestris* pv. *campestris*, RsmA can negatively regulate c-di-GMP levels by binding to and posttranscriptionally regulating multiple *dgc* genes (Lu et al., 2012). In general, CsrA has primarily been found to regulate Dgc and/or Pde enzyme-encoding genes, affecting their function and resulting in alterations to the existing levels of intracellular c-di-GMP. However, an inverse regulatory correlation entailing the indirect c-di-GMP dependent control of CsrA sequestration, resulting in phenotypic variation, has not yet been reported.

Erwinia amylovora is a plant-pathogenic bacterium, causal agent of fire blight disease in apple and pear, and member of the *Enterobacteriaceae* clade (Smits et al., 2017). The EPS amylovoran is a pathogenicity factor in *E. amylovora* Ea1189 and is a critical component of the biofilm matrix within the xylem (Koczan et al., 2009). Amylovoran biosynthesis is functionally dependent on the *ams* operon, comprising 12 genes, *amsG* being the first (Bernhard et al., 1993; Bugert & Geider, 1995). c-di-GMP is a strong positive regulator of amylovoran production as well as *amsG* transcription (Edmunds et al., 2013; Kharadi et al., 2019). However, the pathway by which c-di-GMP regulates *amsG* expression is not fully understood. The RcsBCD phosphorelay is a critical positive regulator of *amsG* expression (Wang et al., 2009, 2012). Feeding into this RcsB-mediated control, CsrA (functionally antagonized by CsrB binding) was found to affect RcsB in *E. amylovora* at a posttranscriptional level, thus indirectly regulating *amsG* transcription (Ancona et al., 2016; Lee et al., 2019; Liu et al., 1997).

We hypothesized that we could decipher the pathway through which c-di-GMP-mediated transcriptional regulation of *amsG* occurs by using an independent transposon mutagenesis approach to identify mutants that were reduced in *amsG* expression under elevated intracellular levels of c-di-GMP. Our results highlight a unique role of CsrD in the c-di-GMP-mediated transcriptional regulation of *amsG* as well as in virulence and biofilm formation.

2 | RESULTS

2.1 | The functional loss of CsrD, under high intracellular c-di-GMP levels, negatively affects *amsG* promoter activity and amylovoran production

The region upstream of *amsG* comprises a predicted transcriptional start site at the −500 bp position (Figure 1a) (Bernhard et al., 1993; Bugert & Geider, 1995). Upstream of the transcriptional start site, an RcsB binding box is located at the −533 to −555 bp position (Figure 1a) (Bernhard et al., 1993; Bugert & Geider, 1995). We cloned a region from *E. amylovora* Ea1189 (2,333,719 to 2,334,519) that includes the *amsG* transcriptional start site, the RcsB binding box, and the sequence upstream of the RcsB box that ends preceding the next consecutive open reading frame (ORF) on the chromosome into the green fluorescent protein (GFP) reporter transcriptional fusion vector pPROBE-NT, generating the construct pPROBE-NT::p*amsG* (Figure 1a). In our previous study, we reported that the combined deletion of all three enzymatically active Pde-encoding genes in *E. amylovora* Ea1189, namely, *pdeA*, *pdeB*, and *pdeC*, resulted in significantly elevated intracellular c-di-GMP levels, amylovoran production, and *amsG* expression levels in vitro (Kharadi et al., 2019). Expression of *gfp* from pPROBE-NT::p*amsG* was significantly elevated in Ea1189Δ*pdeABC* (Figure 1d), and we used this system to find positive regulators of *amsG* transcription via transposon mutagenesis. Tn*5*-based transposon mutants of Ea1189Δ*pdeABC* harbouring pPROBE-NT::p*amsG* were sorted via fluorescent-activated cell sorting with the goal of isolating mutants with an approximately 10- to 100-fold reduction (representative of a graded deviation from the recorded median fluorescence level) in *amsG* promoter activity measured via GFP signal (Figure 1b). Among the sorted mutants, we found three mutants with insertions in the *csrD* ORF, EAM_3136 (Figure 1c).

To study the effect of disrupting CsrD in *E. amylovora*, we deleted *csrD* in Ea1189Δ*pdeABC*. *amsG* promoter activity was significantly reduced in Ea1189Δ*pdeABC*Δ*csrD*, and complementation of this mutant with *csrD* restored *amsG* promoter activity and amylovoran production to the basal levels (Figure 1d,e).

2.2 | *csrD* positively regulates virulence in immature pear and apple shoots

To examine the impact of CsrD on virulence in planta, *csrD* mutants in both wild-type (WT) Ea1189 and Ea1189Δ*pdeABC* backgrounds were assessed for their virulence intensity in immature pear fruitlets and apple shoots. In immature pear fruitlets at 5 days postinoculation (dpi), Ea1189Δ*csrD* showed a significant reduction in necrosis relative to WT Ea1189, and the complementation of the mutant with *csrD* restored WT levels of virulence (Figure 2a). Ea1189Δ*pdeABC*Δ*csrD* was similar to Ea1189Δ*pdeABC* in terms of virulence. However, as previously reported, the significantly elevated levels of c-di-GMP in Ea1189Δ*pdeABC* severely down-regulates expression of type III

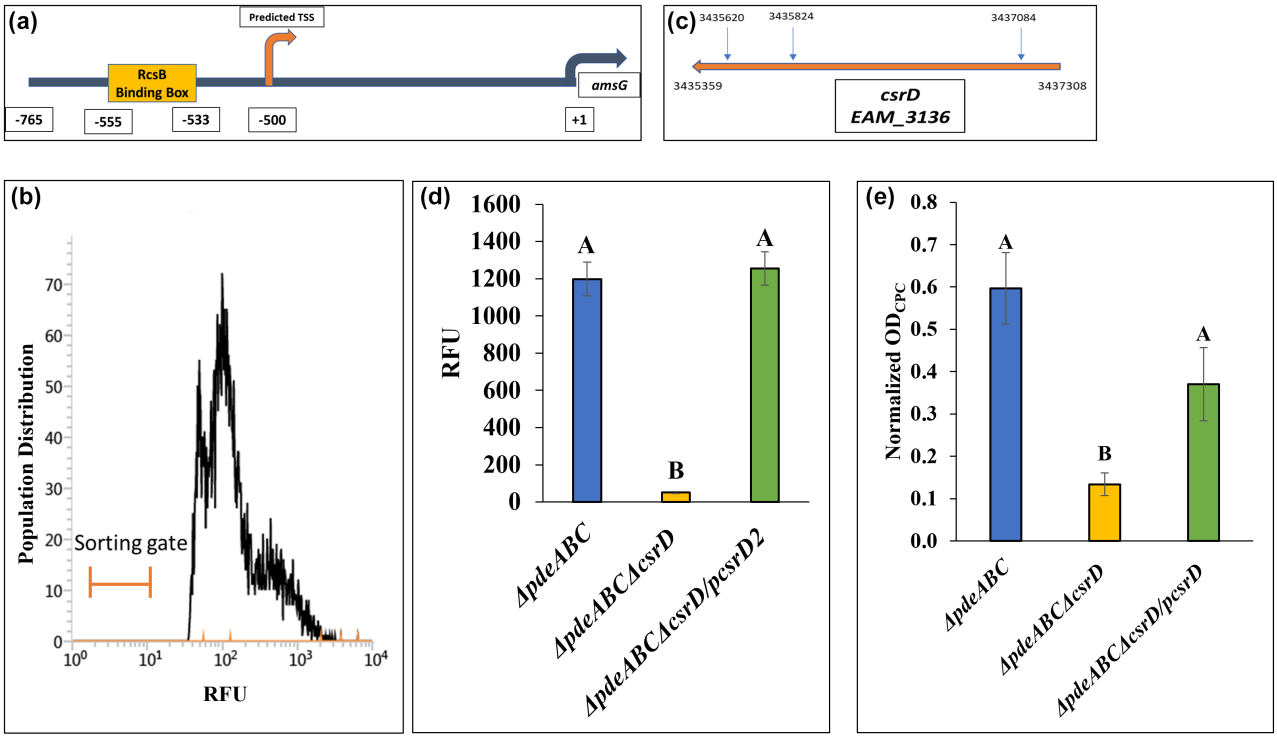

FIGURE 1 (a) A graphical representation of the chromosomal region upstream of *amsG*, including the regulatory components. The *amsG* promoter region comprises a predicted transcriptional start site (TSS) at −500 bp, and the RcsB binding box is located just upstream of the predicted TSS. (b) A collective batch of about 3×10^6 cellular instances of Ea1189Δ*pdeABC*/pPROBE-NT::p*amsG* was obtained using fluorescent-activated cell sorting to screen for mutants with a significant relative reduction in *amsG* promoter activity. The sorting chart depicts the relative distribution of the overall sorted population in terms of relative fluorescence units (RFU), along with the sorting gate set to select mutants in the screening for a reduction in *amsG* promoter activity. (c) A representative map of the Tn*5* insertion sites (vertical arrows) located on *csrD*, relative to the overall chromosomal location of *csrD*. (d) *amsG* promoter activity for Ea1189Δ*pdeABC* and *csrD* mutants and complemented strains (reported via pPROBE-NT::p*amsG*) in both backgrounds determined via flow cytometry 6 h after induction in modified basal medium-A (MBMA) medium. Data presented in the form of RFU for an average of 10,000 cellular instances. (e) Normalized turbidimetric determination of amylovoran production for Ea1189Δ*pdeABC* and Ea1189Δ*csrD* mutants, and complemented strains. All error bars represent standard error of the means. Statistical differences denoted by letters above the bars were calculated based on Tukey's HSD test ($p < 0.05$)

secretion system genes, resulting in reduced necrosis on pear fruitlets (Kharadi et al., 2019). This might account for the lack of a significant reduction in the virulence level of Ea1189Δ*pdeABC*Δ*csrD* relative to Ea1189Δ*pdeABC* (Figure 2a).

In apple shoots, both Ea1189Δ*csrD* and Ea1189Δ*pdeABC*Δ*csrD* showed a reduction in virulence measured as shoot necrosis length at 8 dpi relative to WT Ea1189 and Ea1189Δ*pdeABC*, respectively (Figure 2b). Complementation of both forms of *csrD* mutants restored virulence levels to those of the background strains that the mutants were constructed in (Figure 2b).

2.3 | *csrD* positively regulates biofilm formation under the presence of high intracellular levels of c-di-GMP, but does not itself contribute to c-di-GMP metabolism

To assess the downstream effect of the reduction in amylovoran production due to the deletion of *csrD*, we examined the relative levels of biofilm formation in *csrD* mutants in both WT Ea1189 and Ea1189Δ*pdeABC* backgrounds. It should be noted that the quantitative decline in biofilm formation levels in Ea1189Δ*pdeABC* relative to Ea1189 has been attributed to the high levels of autoaggregation and the consequential impact on physiological and structural changes in cell division and cellular spatial organization observed in Ea1189Δ*pdeABC*; we have characterized this occurrence in our previous studies, and the dependence of autoaggregation on the peptidoglycan hydrolase/metallopeptidase EagA (Kharadi et al., 2019; Kharadi & Sundin, 2019, 2020). With this stipulation, to accurately derive conclusions from this metric, the strainwise comparison of biofilm levels within flow cells has been segregated based on the level of c-di-GMP occurring within WT Ea1189 and Ea1189Δ*pdeABC*. Biofilm formation was not significantly affected in Ea1189Δ*csrD* relative to Ea1189 (Figure 3a,b). However, under high intracellular c-di-GMP conditions, as present in Ea1189Δ*pdeABC*, the deletion of *csrD* resulted in a significant reduction in biofilm formation under flow-based conditions relative to Ea1189Δ*pdeABC* (Figure 3a,b). Additionally, Ea1189Δ*csrD*

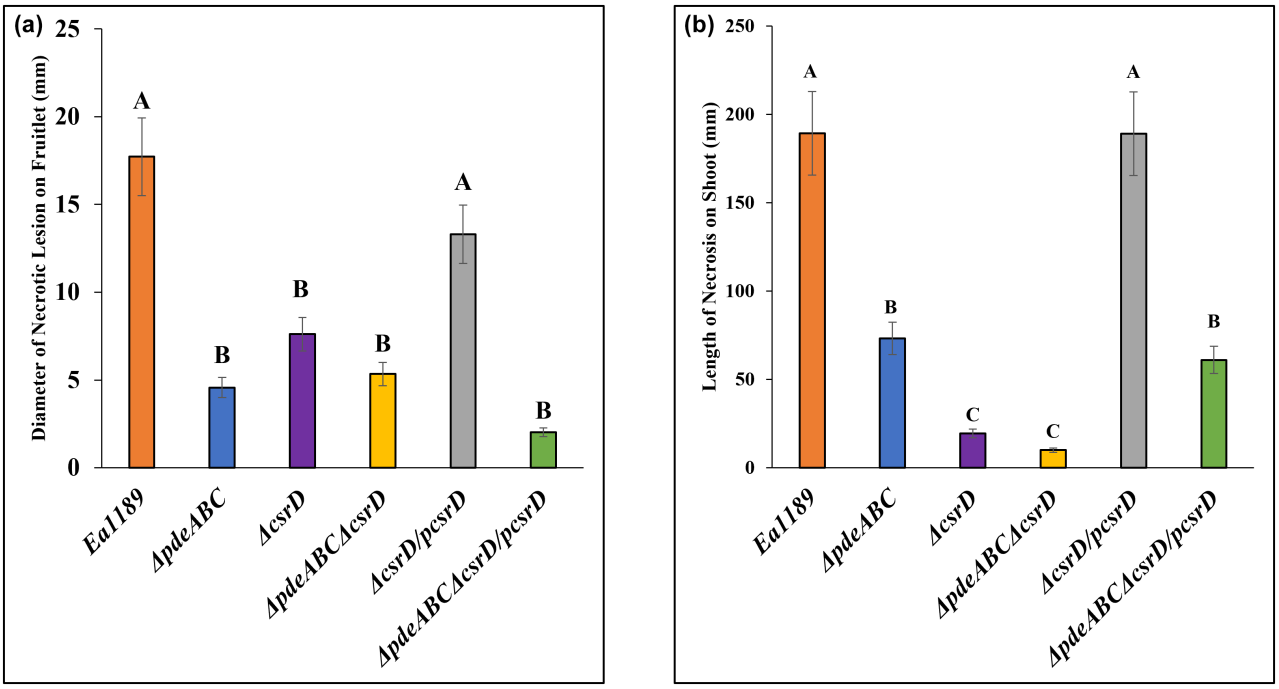

FIGURE 2 Virulence of wild-type *Erwinia amylovora* Ea1189, Ea1189Δ*pdeABC*, and Ea1189*csrD* mutants and complemented strains in both backgrounds on (a) immature pears determined via measuring the diameter of circular necrotic lesions at 5 days postinoculation (dpi) and (b) apple shoots measured in the form of lesion length from the site of inoculation at 8 dpi. All error bars represent standard error of the means. Statistical differences denoted by letters above the bars were calculated based on Tukey's HSD test ($p < 0.05$)

and Ea1189Δ*pdeABC*Δ*csrD* did not show significant differences in terms of intracellular levels of c-di-GMP relative to WT Ea1189 and Ea1189Δ*pdeABC*, respectively (Figure 3c).

2.4 | CsrD binds to c-di-GMP at critical residues within the EAL motif, affecting *amsG* transcription

The domain architecture of CsrD revealed the presence of a GAPES4 (Bobrov et al., 2005) sensory domain in the N-terminal end, flanked by two transmembrane helices, and the C-terminal end contains both a GGDEF and EAL motif (Figure 4a). Aligned CsrD residues from *E. amylovora* (Ea1189) and *E. coli* K12 revealed differences in conserved residues in the GGDEF and EAL motifs (Figure 4a). The amino acid sequence of the *E. amylovora* CsrD EAL motif (highlighted in Figure 4a) contains residues that have been shown to be critical for c-di-GMP binding in other proteins with degenerate EAL domains (Riley et al., 2006; Yu et al., 2020).

CsrD orthologs are present in several members of the *Enterobacteriaceae*, but are not universally distributed (Suzuki et al., 2006). Aligned residues from a subset of these orthologs revealed that the EXLXR motif, critical for c-di-GMP binding, within the EAL domain of these proteins was not entirely conserved, with the L (Leu) residue being the most variable, conserved only in *E. amylovora* and *Photobacterium profundum* (Figure 4b) (Chou & Galperin, 2016). A phylogenetic analysis indicated that the full-length CsrD from *E. amylovora* was most closely related to orthologs from *E. coli*, *Shigella flexneri*, *Salmonella typhimurium*, and *Pectobacterium carotovorum* (Figure 4c).

Pull-down assays using biotinylated c-di-GMP and 6×His-CsrD from *E. amylovora* Ea1189 revealed that c-di-GMP could bind to CsrD with a dissociation constant (K_D) value of c.4 μM (Figure 5a,b,c), as verified by incremental changes to both bait protein and ligand (Figure 5a i, ii). c-di-GMP binding to CsrD was found to be highly specific, as shown in competition experiments. Loss of binding signal was observed on the introduction of unlabelled c-di-GMP as a specific competitor, and was not observed on the introduction of GTP as a nonspecific competitor (Figure 5a iii, iv). While site-directed substitution of critical residues in CsrD (Figure 4a) within the GGDEF motif (residues 308–312, FRSDFAAAAA) did not affect binding to c-di-GMP, substitutions to the EAL motif (combined residues 433–435, EILAAA, and L435A) eliminated c-di-GMP binding in the pull-down assays (Figure 5b) under the conditions tested in the experimental pull-down assays. Both the WT CsrD protein and a truncated version of CsrD that consisted of only the WT EAL domain exhibited binding to c-di-GMP in this assay, but the 6×His-CsrD from *E. coli* K12 did not bind to c-di-GMP (Figure 5b).

Expression levels of *amsG* (normalized by *recA* expression) were elevated, as expected in Ea1189Δ*pdeABC* relative to WT Ea1189 (Figure 6). The deletion of *csrD* in Ea1189Δ*pdeABC* resulted in a significant drop in amylovoran production, which could be restored through the complementation of the native version of *csrD*, as well as the site-directed mutant in the GGDEF domain (p*csrD*308-312A). However, the complementation of Ea1189Δ*pdeABC*Δ*csrD* with the

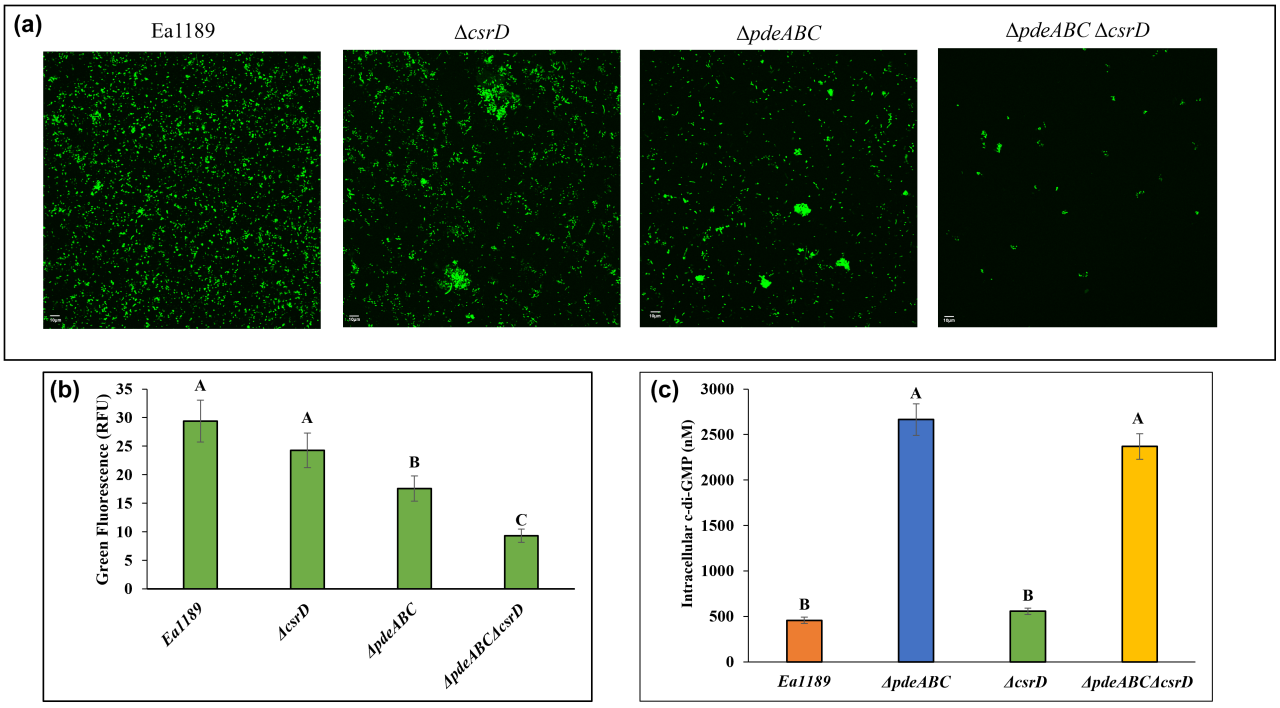

FIGURE 3 (a) Biofilm formation within flow cells determined for wild-type (WT) Ea1189, Δ*pdeABC*, and *csrD* mutants in both backgrounds using green fluorescent protein (GFP)-labelled cells assessed under confocal microscopy. (b) The level of green fluorescence in the flow cell biofilms quantified via ImageJ using the RBG quantification plug-in (Schneider et al., 2012). (c) Intracellular c-di-GMP levels assessed via LC-MS/MS for WT Ea1189, Ea1189Δ*pdeABC*, and Ea1189Δ*csrD* mutants in both backgrounds. All error bars represent standard error of the means. Statistical differences denoted by letters above the bars were calculated based on Tukey's HSD test ($p < 0.05$)

site-directed mutant version of *csrD* in the EAL motif (p*csrD*433-435A) did not restore Ea1189Δ*pdeABC* levels of *amsG* transcription (Figure 6). In conjunction with the effects observed on virulence and amylovoran production, the deletion of *csrD* in WT Ea1189 and the complementation of the *csrD* mutant with an unmodified version of *csrD*, as well as the modified version of *csrD* with site-directed mutations within the GGDEF domain (p*csrD*308-312A) and the EAL motif (p*csrD*433-435A), did not lead to any significant changes in *amsG* expression (Figure 6).

2.5 | CsrD can regulate CsrB degradation in a c-di-GMP dependent manner

In *E. coli*, CsrD has been demonstrated to be a specificity factor for RNase E, which can direct RNase E towards the targeted degradation of the sRNA CsrB (Suzuki et al., 2006). In *E. amylovora*, we found that the loss of RNase E (encoded by *rne*) and *csrD* resulted in a significant increase in CsrB transcript levels relative to WT Ea1189 (Figure 7a). While complementation of the mutants with *rne* and *csrD*, respectively, was able to restore transcript levels comparable to WT, Ea1189Δ*csrD* complemented with the EAL motif mutated version of *csrD* (433-435A) retained the high levels of CsrB transcripts (Figure 7a). In Ea1189Δ*pdeABC*, a significant decrease in CsrB transcripts was observed relative to Ea1189. The loss of both *csrD* and *rne* in Ea1189Δ*pdeABC* resulted in a significant increase in CsrB transcript levels compared to Ea1189Δ*pdeABC*, and complementation of these mutant strains with *csrD* and *rne*, respectively, enabled the recovery of CsrB levels comparable to Ea1189Δ*pdeABC* (Figure 7a). However, Ea1189Δ*pdeABC*Δ*csrD* complemented with the EAL motif mutated version of *csrD* (433-435A) still had high levels of CsrB transcripts (Figure 7a). To study the effect of both CsrD and c-di-GMP on the degradation of CsrB, we used the *E. amylovora* strain Ea1189Δ12, which lacks all the functionally active/inactive Dgc and Pde enzyme-encoding genes, including *csrD*, and does not produce any intracellular c-di-GMP (Kharadi et al., 2021). We confirmed that *csrD* expression was not significantly different in WT Ea1189 as compared to Ea1189Δ12 complemented with *csrD* and *csrD* (433-435A) (Figure S1). Thus, using Ea1189Δ12, we were able to selectively control for the presence or absence of c-di-GMP to then study the interactive effect with CsrD.

Prior to investigating the degradation dynamics of CsrB, we determined the basal levels of CsrB transcripts in our strains. Levels of CsrB were significantly lower in Ea1189Δ12/p*csrD*/*pdgcOE* compared to in Ea1189Δ12, whereas Ea1189Δ12/p*csrD*(433-435A)/*pdgcOE* and Ea1189Δ12/p*csrD* had CsrB levels that were similar to Ea1189Δ12 (Figure 7b). It must be noted that we used actively growing subcultures for all the strains that were grown in media amended with isopropyl β-D-1-thiogalactopyranoside (IPTG) as appropriate, which would then be reflected in the ongoing process of CsrB generation and degradation, resulting in differences in the transcript levels of the sRNA at any given time. Next, independent

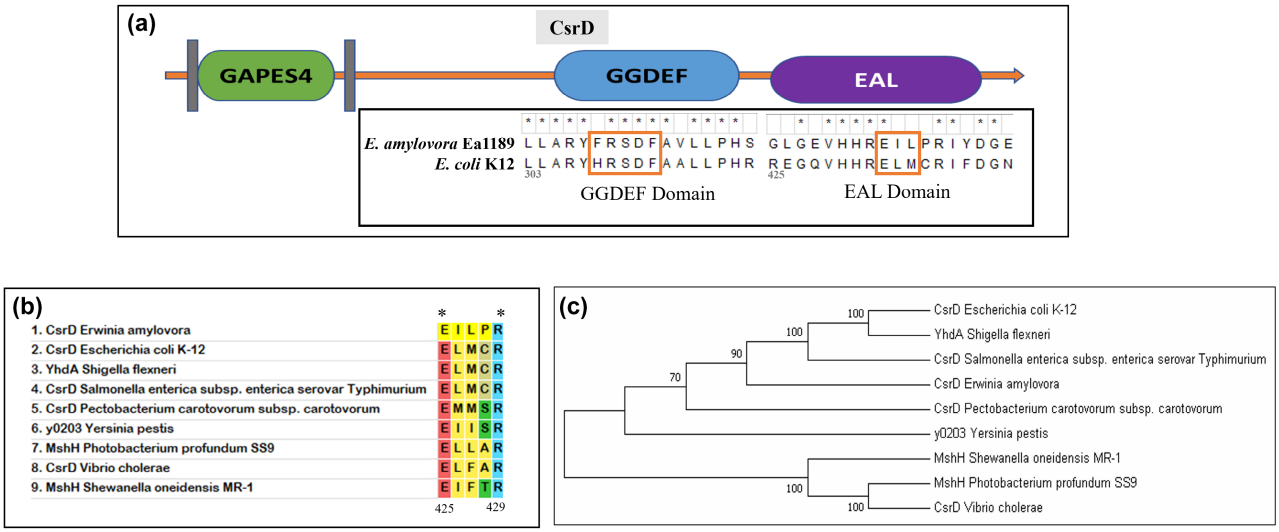

FIGURE 4 (a) The domain architecture of CsrD comprises an N-terminal GAPES4 periplasmic sensory domain flanked by transmembrane helices. CsrD also comprises GGDEF and EAL motifs (Finn et al., 2014). Critical residues for each domain are highlighted to denote the variations present in *Erwinia amylovora* Ea1189 versus *Escherichia coli* K12 when aligned. (b) Aligned CsrD orthologs from a diverse subset of *Enterobacteriaceae* species indicate that the EXLXR motif within the EAL domain of CsrD is only conserved in the Glu (E) and Arg (R) residues. The Leu (L) residue was found to be highly variable among the evaluated species. Alignment was conducted using Clustal Omega (Sievers & Higgins, 2014). (c) A maximum-likelihood tree (Schmidt et al., 2002) revealed three distinct lineages within the evaluated CsrD orthologs from various *Enterobacteriaceae* species. The functionally active PdeC from *E. amylovora* was used as an out-group. MEGA v. 7.0 was used as a platform to conduct both analyses (Agbo et al., 2003)

of the basal levels of CsrB present in the strains, we tracked the relative levels of CsrB degradation at various time points after rifampicin was added to cultures to inhibit RNA polymerase and found that, relative to Ea1189Δ12, Ea1189Δ12/p*csrD* exhibited significantly reduced CsrB transcript levels at the 30 min time point, but not at earlier time points (Figure 7c). The overexpression of a Dgc from *Vibrio cholerae* in Ea1189Δ12/p*csrD*/*pdgcOE* led to a consistently significant decrease of CsrB transcript levels, as quantified by both reverse transcription-quantitative PCR (RT-qPCR; 5, 20, and 30 min samples) and northern blot analyses (30 min sample), relative to all other sample types (Figure 7d). Use of a modified version of *csrD* to complement Ea1189Δ12 in the strain Ea1189Δ12/p*csrD*(433-435A)/p*dgcOE* did not result in increased CsrB degradation relative to Ea1189Δ12 (Figure 7c,d).

3 | DISCUSSION

In this study, we demonstrated that the binding of c-di-GMP within the EAL domain of *E. amylovora* CsrD enhances the degradation of the sRNA CsrB mediated by RNase E, thus potentially alleviating the sequestration of CsrA, enabling CsrA to function with the RcsBCD phosphorelay in the positive regulation of the amylovoran biosynthetic operon mediated through RcsB binding at the *amsG* promoter (Ancona et al., 2016; Wang et al., 2012). While the Csr and Rsm systems have been reported to manipulate intracellular levels of c-di-GMP via regulating the expression of Dgc and Pde enzymes involved in the synthesis and degradation of c-di-GMP (Jonas et al., 2010), CsrD in *E. amylovora* represents an evolutionary divergence in function in which the Csr system is responsive to c-di-GMP, resulting in regulation that increases the expression of a critical EPS biosynthetic operon.

In *E. coli*, it has been demonstrated that CsrD can regulate turnover of the sRNAs CsrB and CsrC by directing RNase E target specificity (Suzuki et al., 2006). While the activity mediated by CsrD was not linked to c-di-GMP metabolism, the GGDEF and EAL domains were found to be essential for enzymatic activity towards the sRNA CsrB/C and in directing RNase E specificity (Suzuki et al., 2006). The degenerate EAL domain of CsrD has emerged as a key site for post-translational stimulation of CsrD activity. In *E. coli*, this domain can specifically bind unphosphorylated $EIIA^{Glc}$, linking CsrD activity to the presence of the preferred carbon source glucose (Leng et al., 2016). Binding of the CsrD homolog MshH to unphosphorylated $EIIA^{Glc}$ has also been demonstrated in *V. cholerae*, although the effect of this binding on MshH function has not been fully assessed (Pickering et al., 2012). Distinct from this regulatory structure present in *E. coli*, we found that the *eIIA* mutant in *E. amylovora* did not exhibit any significant changes in amylovoran production or *amsG* expression (data not shown). We hypothesize that this lack of linkage of CsrD with glucose availability may be because *E. amylovora* is rarely exposed to glucose during its life cycle. During most of its life cycle, *E. amylovora* is located within the interior of its Rosaceae family plant host, where cells are mainly exposed to sorbitol and sucrose, the two predominant sugars present in these hosts (Petanidou, 2005).

This current study and our previous study involving the overall analysis of all c-di-GMP metabolic enzymes in *E. amylovora* have consistently indicated that the GGDEF and EAL domains in CsrD

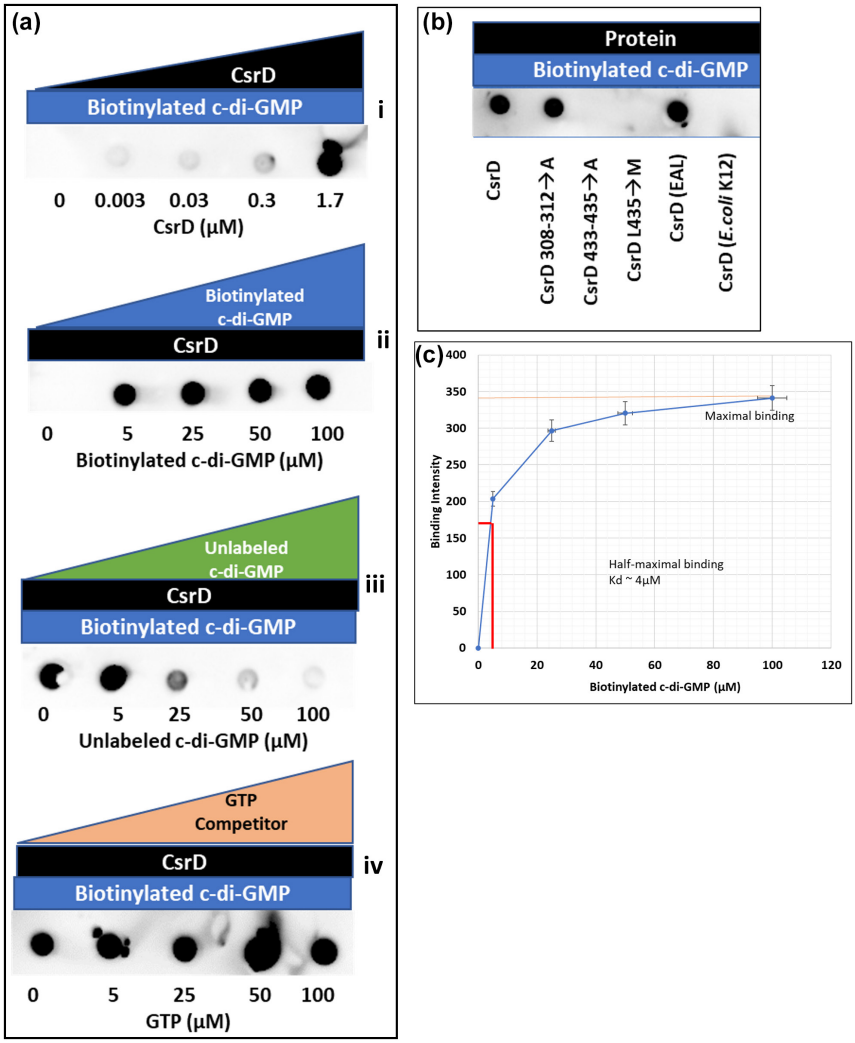

FIGURE 5 (a) A panel depicting the overall results of pull-down assays with multiple variations analysed to determine the specifics of CsrD binding to c-di-GMP. (i) Biotinylated c-di-GMP (100 μM) immobilized to streptavidin beads shows binding to increasing concentrations (0, 0.003, 0.03, 0.3, 1.7 μM) of His-tagged CsrD. (ii) Binding between 1.7 μM of CsrD and increasing concentrations (0, 5, 25, 50, 100 μM) of biotinylated c-di-GMP. (iii) Binding between 1.7 μM CsrD and 100 μM biotinylated c-di-GMP with increasing concentrations (0, 5, 25, 50, 100 μM) of unlabelled c-di-GMP as a competitor. (iv) Binding between 1.7 μM CsrD and 100 μM of biotinylated c-di-GMP with increasing concentrations (0, 5, 25, 50, 100 μM) of GTP as a nonspecific competitor. (b) Binding between truncated and site-directed substituted versions of *Erwinia amylovora* CsrD as well as CsrD from *Escherichia coli* K12 (1.7 μM of all proteins) and biotinylated c-di-GMP (100 μM). (c) The dissociation constant (K_D) for CsrD binding to c-di-GMP determined at the half-maximal binding level (Chambers & Sauer, 2017). The graph compares the binding level in the form of pixel density from the immunoblot (generated using ImageJ) involving a pull-down of the interaction between 1.7 μM of CsrD with increasing concentrations of biotinylated c-di-GMP (Schneider et al., 2012)

are not functionally active in c-di-GMP metabolism (Kharadi et al., 2021). However, proteins in other systems that contain degenerate GGDEF or EAL domains have been found to bind c-di-GMP and serve as c-di-GMP receptors, which can impact their functional activity (Romling et al., 2013). The EXLXR motif within the EAL domain is a critical target site for monomeric c-di-GMP binding (Barends et al., 2009; Minasov et al., 2009; Tchigvintsev et al., 2010). Proteins with functionally degenerate EAL domains have been found to retain the EXLXR motif for the purpose of c-di-GMP binding (Guzzo et al., 2013; Navarro et al., 2009, 2011). For example, in *X. oryzae*, the FimX-like protein FilP was shown to be able to bind c-di-GMP within a degenerate EAL domain, and c-di-GMP binding was linked to its ability to interact with a PilZ domain-containing protein PXO_02715 and affect virulence through the type III secretion system (Yang et al., 2014).

Within the EXLXR motif, the central Leu residue (L) is critical to stabilize the overall binding with the ribose-phosphate ring structure. A comparison of the CsrD orthologs in a diverse subset of *Enterobacteriaceae* also indicated that this Leu residue is highly variable (Figure 4b). Our results indicate that the truncated version of CsrD comprising the EAL domain retains c-di-GMP binding, thus implicating this domain in the locational binding specificity of c-di-GMP towards CsrD. Also, the L435 residue, located within the canonical EXLXR motif (located at residues 433–437) in *E. amylovora* CsrD,

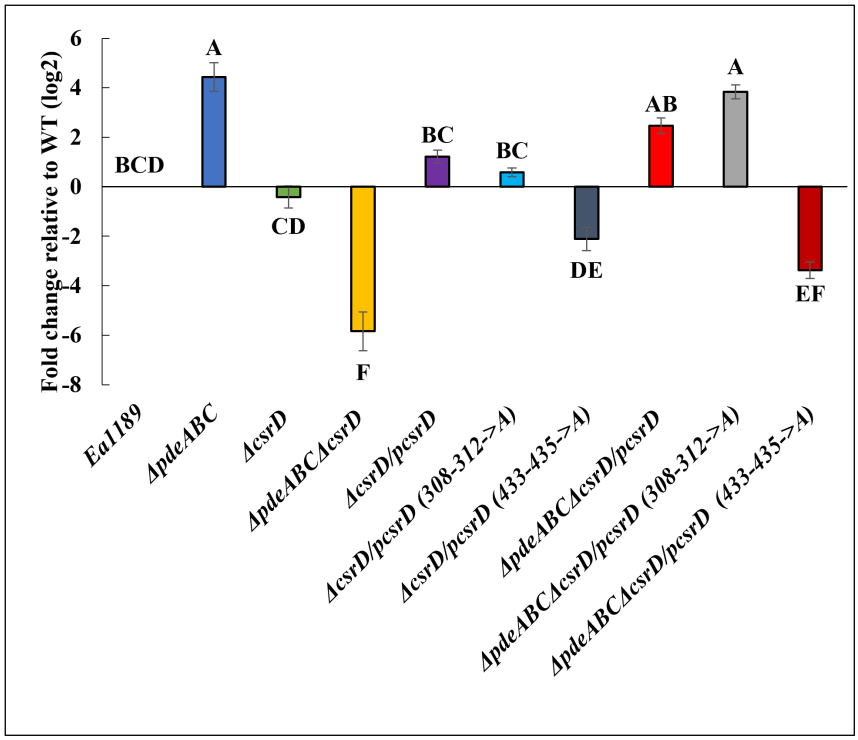

FIGURE 6 Relative fold change in *amsG* expression for *Erwinia amylovora* wild-type (WT) Ea1189, Ea1189Δ*pdeABC*, *csrD* mutants, and mutant strains complemented with native and modified versions of *csrD* in Ea1189 and Ea1189Δ*pdeABC* backgrounds 6 h after induction in MBMA medium. Error bars represent standard error of the means. Statistical differences denoted by letters above the bars were calculated based on Tukey's HSD test ($p < 0.05$)

was critical for c-di-GMP binding. Mutations to another subregion of this motif (433-435A) also functionally abolished both binding to c-di-GMP as well as the downstream impact of c-di-GMP-bound CsrD on *amsG* transcription. To conduct a comparative analysis, we changed the L435 residue to Met (M) because the CsrD originating from *E. coli* K12 had this substitution at the position. Both *E. amylovora* CsrD (with L435M) as well as CsrD from *E. coli* K12 did not show any detectable binding to c-di-GMP. We determined that the dissociation constant for c-di-GMP binding to CsrD was about 4 μM. In a biological context, c-di-GMP levels recorded in WT Ea1189 are below this binding threshold. However, this does not preclude binding of c-di-GMP by CsrD during *E. amylovora* infection and is probably a reflection of our inability to measure c-di-GMP levels in *E. amylovora* during disease progression within the host, compounded by the potential of localized c-di-GMP signalling within the cell for specific functionality (Christen et al., 2010; Hengge, 2021).

The controlled modulation of intracellular c-di-GMP levels enables *E. amylovora* to transition from using the type III secretion system to biofilm formation as the primary virulence strategy in planta (Kharadi & Sundin, 2021). However, there are limited tools available to resolve c-di-GMP concentrations at a cellular level in planta during disease occurrence (Hengge, 2021; Jenal et al., 2017). Developing tools to track the variation in c-di-GMP levels in *E. amylovora* during disease progression will be critical to fully understand the functional relevance of CsrD regulation. We hypothesize that the deviation from the dependence on the GGDEF domain for CsrD function, as is the case in *E. coli*, is due to the structural implications of c-di-GMP binding to the EXLXR motif in terms of the overall functional complex of CsrD, RNase E, and the target sRNA. However, further research into the thermodynamic differences in the function of such a complex in the presence and absence of, as well as modulating levels of c-di-GMP will be needed to gain clarity in this regard.

Our findings indicate that even under conditions where c-di-GMP is absent from the cell, CsrD improves the efficiency of CsrB degradation mediated by RNase E. However, the additional presence of c-di-GMP significantly improves the efficiency of CsrB degradation. We also found that this additive effect of c-di-GMP in terms of downstream CsrB degradation did not result from any

FIGURE 7 (a) Relative fold change in sRNA CsrB expression for *Erwinia amylovora* wild-type Ea1189, Ea1189Δ*pdeABC*, *csrD*, *rne* mutants, and mutant strains complemented with native and modified versions of *csrD* in Ea1189 and Ea1189Δ*pdeABC* backgrounds 6 h after induction in MBMA medium. Error bars represent standard error of the means. Statistical differences denoted by letters above the bars were calculated based on Tukey's HSD test ($p < 0.05$). (b) Relative transcript levels of *CsrB* (prior to the addition of rifampicin for the degradation assay) determined via reverse transcription-quantitative PCR (RT-qPCR) for Ea1189Δ12 transformed with native and modified forms of p*csrD* and/or p*dgcOE* relative to Ea1189Δ12. Error bars represent standard error of the means. Statistical differences denoted by asterisks above the bars were calculated based on Student's *t* test relative to Ea1189Δ12 for all strain variants ($p < 0.05$). (c) Transcript degradation study over time for *csrB* in *E. amylovora* Ea1189Δ12 and Ea1189Δ12 transformed with native and modified forms of p*csrD* and/or p*dgcOE*, conducted via RT-qPCR and (d) northern blot analysis. For the RT-qPCR results, error bars represent standard error of the means. Statistical differences denoted by asterisks at datapoints were calculated based on Student's *t* test relative to Ea1189Δ12 at each time point for all strain variants ($p < 0.05$)

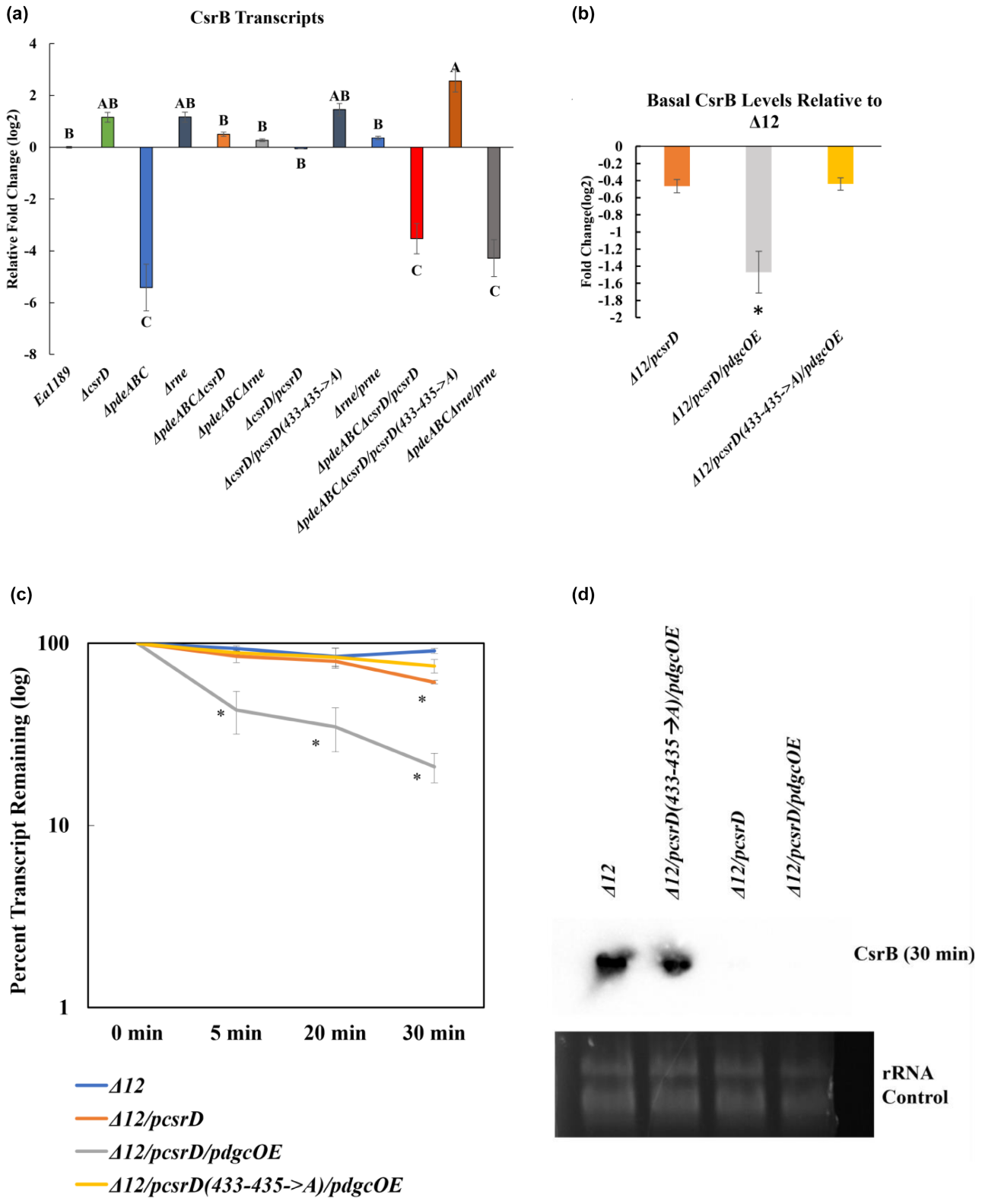

transcriptional impact of c-di-GMP on *csrD* itself, rather from the interaction between c-di-GMP and CsrD. In other systems, c-di-GMP can bind to proteins at degenerate EAL domains, such as in the protein FimX in *X. campestris*, and this enables the protein to interact with PilZ, which would otherwise not be possible due to variations in the molecular size and structure of these two proteins (Chin et al., 2012; Guzzo et al., 2013). RNase E-mediated degradation of sRNAs is understood to occur through two separate mechanisms for Hfq-dependent and -independent sRNAs. RNase E cleavage sites on CsrB (RsmZ) have been identified in *Pseudomonas fluorescens* (Duss et al., 2014). Both CsrD and RapZ are thought to function through specifically binding to sRNAs and modifying their structure to make them vulnerable to degradation by RNase E (Gonzalez et al., 2017; Suzuki et al., 2006; Vakulskas

et al., 2016). While our study did not focus on the functional dynamics of CsrA due to the pleiotropic effects resulting from *csrA* deletion in *E. amylovora*, further research will be needed to understand if c-di-GMP binding to CsrD changes the dynamics of the interaction of CsrD with RNase E or if this process changes the susceptibility to cleavage of the CsrA–CsrB bound complex (Suzuki et al., 2006; Vakulskas et al., 2016).

The EPS amylovoran is a critical pathogenicity determinant in *E. amylovora* in both the initial type III secretion system-mediated phase of infection that manifests within the apoplast region in flowers and in leaves at shoot tips, as well as during the biofilm formation phase in the xylem vasculature of the apple host (Koczan et al., 2009; Zhao et al., 2009). The physical and quantitative elevation in amylovoran production is evident in the apoplast–xylem transition (Koczan et al., 2009; Smits et al., 2017). Our results suggest that c-di-GMP-elevation-based modification of CsrB levels result in elevated *amsG* transcription, which primarily coincides with the apoplast–xylem transition because this particular transition has also been correlated with increased c-di-GMP production to initiate biofilm formation (Kharadi et al., 2021; Kharadi & Sundin, 2019). Furthermore, because amylovoran production is constitutive in *E. amylovora*, the threshold of amylovoran levels needed to facilitate biofilm maturation might be significantly higher (Koczan et al., 2009). Thus, we hypothesize that a targeted increase in amylovoran production has evolved due to the presence of elevated levels of available c-di-GMP substrate, which allows for binding to CsrD. This dichotomy is reflected in our observations in the form of reduced virulence on the loss of *csrD* under both native and elevated levels of c-di-GMP (occurring within WT Ea1189 and Δ*pdeABC*, respectively) in apple shoots (and not in the pear fruitlet system) wherein the shift towards the biofilm formation is critical for disease progression. This indicates that the temporal elevation in c-di-GMP levels during the shift to biofilm formation channelled through the effect of CsrD on amylovoran production is present in WT Ea1189 and exacerbated in Ea1189Δ*pdeABC* due to its inability to efficiently degrade intracellular c-di-GMP, as corroborated through in vitro biofilm development within flow cells as well as virulence in planta. In an evolutionary context, minor modifications can result in the development of c-di-GMP binding affinity in a protein and, in many cases, spatial separation and the dissociation constant and activation constant of the protein towards c-di-GMP can help regulate signalling activity (Chou & Galperin, 2016; Hengge, 2021; Jenal et al., 2017). However, due to limitations in being able to visually track bacterial movement and intracellular c-di-GMP changes during infection in planta, we are currently unable to directly document this mode of EPS regulation dependent on c-di-GMP in *E. amylovora*.

A collective analysis of the role of EPS biosynthesis in other bacterial pathogens, including *Pseudomonas aeruginosa*, *E. coli*, *V. cholerae*, and *S. typhimurium*, suggests that EPS production often enhances host colonization, but is not strictly a pathogenicity factor, or has a constitutive presence, as amylovoran does in *E. amylovora* (Amarasinghe et al., 2013; Ebel & Trempy, 1999; Gervais et al., 1992; Hentzer et al., 2001; Koczan et al., 2009; Ledeboer & Jones, 2005; Nadell & Bassler, 2011; Zhang et al., 2008). Additionally, the level of diversity in the multifactorial control of amylovoran is also unique to *E. amylovora*. This indicates that the need to consistently maintain and specifically modify/elevate amylovoran production is a limiting factor in terms of successful host colonization.

Overall, the regulatory model that can be inferred through our findings includes two conditional variants (Figure 8). In the presence of low intracellular levels of c-di-GMP, the efficiency of the degradation of CsrB mediated through CsrD (in conjunction with RNase E) is greatly diminished. This potentially allows for the elevated sequestration of CsrA by increased levels of CsrB, resulting in the potential decline of CsrA-mediated posttranscriptional interaction with *rcsB*, as well as its suppressive activity towards Lon protease (which can target RcsB), eventually leading to reduced *amsG* transcription. Our evidence corroborates this through the demonstration of the correlation of CsrD presence (with high and low levels of c-di-GMP) with CsrB degradation. In the other conditional variant, the generation of elevated levels of c-di-GMP within the cell can lead to CsrD being bound to c-di-GMP, which enhances CsrB degradation through RNase E. The reduced levels of CsrB allow for a potential increase in efficient posttranscriptional interaction between CsrA and *rcsB* owing to the presence of elevated levels of unbound CsrA as well as the restoration of CsrA-based decrease of Lon protease activity towards RcsB (Ancona et al., 2016; Lee et al., 2018, 2019). Together, this can result in elevated levels of *amsG* transcription, with a downstream impact on amylovoran biosynthesis.

We thus present evidence of a novel, evolutionarily divergent function of CsrD in its ability to bind c-di-GMP through critical residues in its otherwise enzymatically inactive EAL domain. This property allows for the timed control of EPS generation through CsrB/CsrA to facilitate virulence progression in *E. amylovora*.

4 | EXPERIMENTAL PROCEDURES

4.1 | Bacterial strains, plasmids, and growth conditions

All bacterial strains and vectors used in this study and their relevant characteristics are listed in Table 1. Relevant primer descriptions and sequences are listed in Table S1. *E. amylovora* and *E. coli* strains were grown in Luria-Bertani (LB) medium unless otherwise noted. Strains were grown in MBMA amended with 1% sorbitol (Edmunds et al., 2013) when measuring amylovoran production, *amsG* expression, and treating cells for cell sorting or flow cytometry. Media were amended with ampicillin (Ap; 100 μg/ml), chloramphenicol (Cm; 10 μg/ml), gentamicin (Gm; 10 μg/ml), kanamycin (Km; 100 μg/ml), or tetracycline (Tc; 10 μg/ml), and with 1 mM IPTG for any overexpression vectors, as appropriate.

4.2 | Bioinformatics

The *E. amylovora* Ea1189 and *E. coli* K12 genome sequences along with annotations were acquired from the National Center for

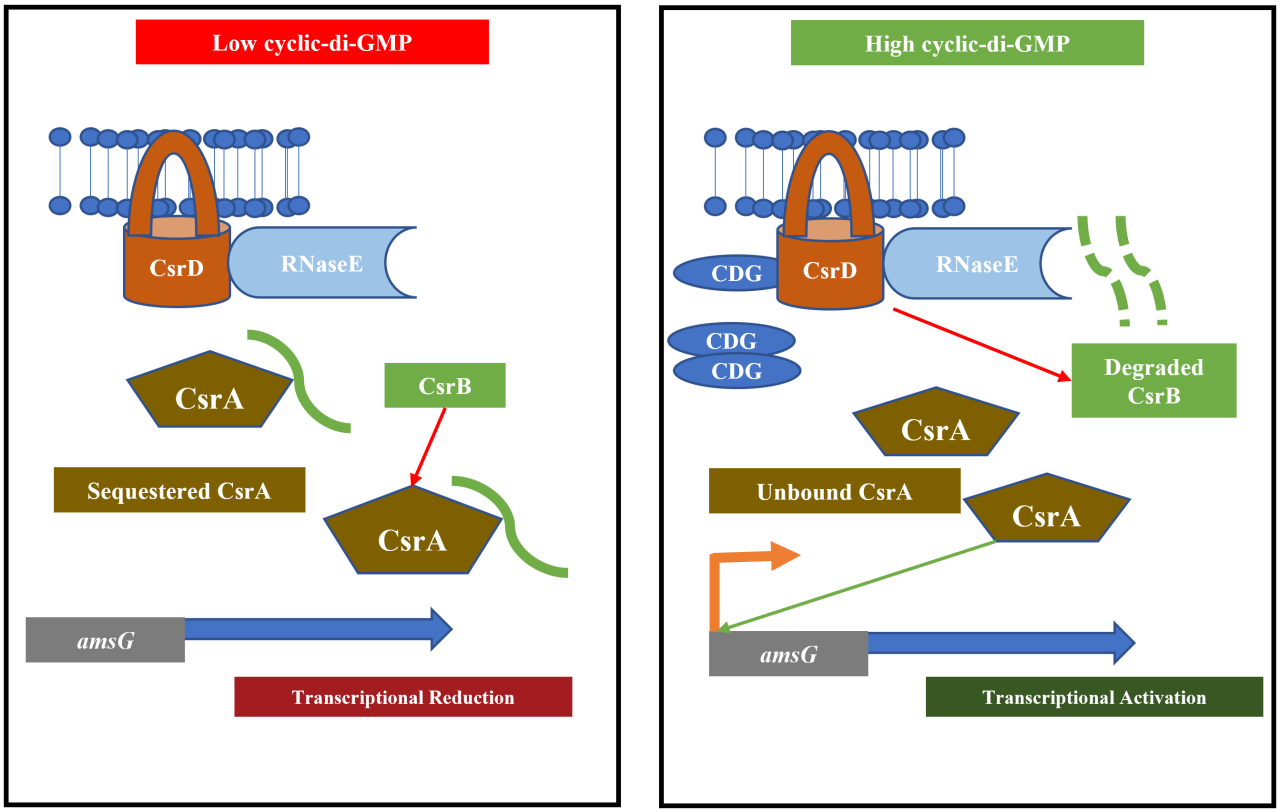

FIGURE 8 A schematic overview of the multicomponent regulatory cascade that affects *amsG* transcription in *Erwinia amylovora*. Under relatively low intracellular levels of c-di-GMP, reduced degradation of CsrB can lead to increased availability to bind to and sequester CsrA, thereby potentially reducing its interaction with *rcsB* (at a posttranscriptional level), as well as its suppressive activity towards Lon protease, thus hindering the positive transcriptional regulation of *amsG* mediated by RcsB. With increasing intracellular levels of c-di-GMP, CsrD bound to c-di-GMP can positively affect RNase E degradative activity towards CsrB. This could result in elevated levels of unbound CsrA freely interacting with *rcsB* and suppressing Lon protease, thus leading to a positive impact on *amsG* transcription

Biotechnology Information (NCBI) (Riley et al., 2006; Yu et al., 2020). Artemis (Java) was used to browse the genome (Carver et al., 2012). The NCBI BLAST (Johnson et al., 2008) tool was used to detect transposon insertion sites in *E. amylovora*. Pfam v. 32.0 (Finn et al., 2014) was used for motif annotation in the proteins of interest. MEGA v. 7.0 (Agbo et al., 2003) was used for protein/DNA alignments.

Previously characterized CsrD ortholog amino acid sequences from specific *Enterobacteriaceae* species were acquired from NCBI (Suzuki et al., 2006). Sequence alignment was conducted using Clustal Omega in MEGA v. 7.0 (Sievers & Higgins, 2014). Maximum-likelihood (1000 bootstrap replicates) phylogenetic tree construction with PdeC from *E. amylovora* as an outgroup representing a functionally active Pde enzyme was conducted using MEGA v. 7.0.

4.3 | Genetic manipulations and analysis

DNA manipulations were conducted using standard protocols (Sambrook et al., 2001). The λ-red recombinase system was used to generate chromosomal deletion mutants (Datsenko & Wanner, 2000). The promoter region of *amsG* was cloned into pPROBE-NT (Miller et al., 2000) to generate a GFP-based transcriptional fusion reporter used for both cell sorting and flow cytometry-based relative gene expression measurements. *csrD*, along with its native promoter, was cloned into pBBR1-MCS5 and/or pACYCDuet-Site1 (Novagen) for complementation studies. The ORF for *csrD* (truncated) was cloned into pET21-a (Novagen) for protein extraction via induced overexpression. Site-directed substitutions on both these vector constructs were conducted using a QuickChange kit (Agilent).

4.4 | Transposon mutagenesis and mutant screening

Transposon mutagenesis was conducted using biparental mating with *E. amylovora* Ea1189Δ*pdeABC* (with pPROBE-NT::p*amsG*) and *E. coli* S17 carrying Tn*5*-B30, as previously described (Erickson et al., 2016; Simon et al., 1989). Transposon mutants were suspended in MBMA for 6 h and were processed via an influx cell sorter (BD Biosciences) fitted with a 530/40 nm filter for GFP. Selected mutants (based on assigned channel gates) were sorted into individual wells in a 96-well plate containing LB medium. Mutants were grown for 24 h at 28°C. An arbitrary PCR-based approach, as previously described (Lauro et al., 2008), was used to locate the transposon insertion sites, confirmed by Sanger sequencing.

TABLE 1 Bacterial strains, plasmids, and their relevant characteristics

Bacterial strain or plasmid	Relevant characteristics	References
Erwinia amylovora strains		
Ea1189	Wild type	Edmunds et al. (2013)
Ea1189Δ*csrD*	*csrD* deletion mutant	This study
Ea1189Δ*pdeABC*	*pdeA*, *pdeB* and *pdeC* deletion mutant	Kharadi et al. (2019)
Ea1189Δ*pdeABC*Δ*csrD*	*csrD*, *pdeA*, *pdeB*, and *pdeC* deletion mutant	This study
Ea1189Δ12	Total c-di-GMP systemic deletion mutant	Kharadi et al. (2021)
Escherichia coli strains		
S17-1	Strain carrying transposon Tn*5*-B30 which confers tetracycline resistance to the recipient strain; Tc^R	Simon et al. (1989)
BL21(DE3)	Strain for IPTG-induced expression of T7 promoter-based vectors for recombinant proteins	Invitrogen
Plasmids		
pKD3	Cm^R cassette flanked by FRT sites; Cm^R	Datsenko and Wanner (2000)
pKD46	L-Arabinose-inducible lambda red recombinase; Ap^R	Datsenko and Wanner (2000)
pTL18	IPTG-inducible FLP recombinase; Tc^R	Long et al. (2009)
pMP2444	pBBR1MCS-5 with *gfp* under *lac* promoter; Gm^R	Stuurman et al. (2000)
pPROBE-NT	Broad-host range GFP-reporter transcriptional fusion cloning vector pBBR backbone *ori*; Km^R	Miller et al. (2000)
pBBR1-MCS5	Broad-host range cloning vector pBBR *ori*; Gm^R	Kovach et al. (1995)
pACYC-Duet-1	Expression vector containing two multiple cloning sites: P15A *ori*; Cm^R	Novagen
pET28-a	Bacterial expression vector with T7 *lac* promoter with LacI repressor site; Km^R	Novagen
pEVS143	Broad-host-range, IPTG-inducible (*ptac*) cloning vector; inducible Cm^R and GFP; Km^R	Dunn et al. (2006)
pPROBE-NT::p*amsG*	Promoter region of *amsG* (ending at −765 bp upstream of *amsG*) in pPROBE-NT; Km^R	This study
p*csrD*	*csrD* with native promoter in pBBR1-MCS5; Gm^R	This study
p*csrD2*	*csrD* with native promoter in pACYC-Duet1; Cm^R	This study
p*csrD* 308-312A	p*csrD* backbone with site-directed mutations in CsrD residues 308–312 FRSDFAAAAA; Gm^R	This study
p*csrD* 433-435A	p*csrD* backbone with site-directed mutations in CsrD residues 433–435 EILAAA; Gm^R	This study
pRRK13	*csrD* open reading frame (ORF) excluding transmembrane motifs (from residue 153) with an N-terminal 6×His-tag cloned in pET28-a; Km^R	This study
pRRK14	pRRK13 backbone with site-directed mutations in CsrD residues 308–312 FRSDFAAAAA; Km^R	This study
pRRK15	pRRK13 backbone with site-directed mutations in CsrD residues 433–435 EILAAA; Km^R	This study
pRRK16	pRRK13 backbone with site-directed mutations in CsrD residues L435M; Km^R	This study
pRRK17	*csrD* ORF truncated to include the EAL domain (residues 403–633) with an N-terminal 6×His-tag cloned in pET28-a; Km^R	This study
pRRK18	*csrD* (*E. coli* K12) ORF excluding transmembrane motifs (residue 153) with an N-terminal 6×His-tag cloned in pET28-a; Km^R	This study
p*dgcOE*	*Vibrio cholerae* gene VCA0956 in pEVS143; Km^R	Waters et al. (2008)

4.5 | Flow cytometry

Strains were grown overnight in LB medium at 28°C, followed by a 6-h induction in MBMA. Relative promoter activity for *amsG* (using pPROBE-NT::p*amsG*) was measured in the strains using an LSRII instrument (BD Biosciences) fitted with an FL3 filter at 530/30 nm for GFP measurement. An average of 10,000 cellular instances was measured for each strain. Analysis was conducted using Flowing software v. 2.5.1 (University of Turku, Finland).

4.6 | Amylovoran production measurement

Amylovoran production was measured using a turbidometric assay, as previously described (Edmunds et al., 2013). Overnight cultures grown at 28°C were normalized (OD_{600}) and subcultured in MBMA for 48 h. The relative amylovoran concentration in the culture supernatants was measured using cetylpyridinium chloride (CPC) (50 mg/ml) with an incubation time of 10 min. The data has been presented in the form of the OD_{600} of CPC binding normalized by the cell density. Statistical analysis, including Tukey's honestly significant difference (HSD), was conducted using JMP statistical software.

4.7 | Virulence assays

Immature cv. Bartlett pear fruitlets were stab-inoculated as previously described (Kharadi et al., 2019). Strains were grown overnight and adjusted to a concentration of 10^4 cfu/ml. Following inoculation, the pear fruitlets were incubated for 5 dpi at 28°C. Infection levels were quantified in the form of the diameter of circular necrotic lesions surrounding the point of inoculation. Apple (*Malus* × *domestica* 'Gala') shoots were cut-inoculated as previously described (Kharadi et al., 2019). Strains were grown overnight and normalized to an OD_{600} of 0.8. Young shoot tips on apple trees were cut using scissors dipped in bacterial inoculum. Relative measurement of virulence was collected in the form of necrotic tissue/shoot blight length from the point of inoculation at 8 dpi. Statistical analysis, including Tukey's HSD, was conducted using JMP statistical software.

4.8 | Biofilm formation in flow cells

Relative levels of biofilm development were assessed using flow cells (Kharadi & Sundin, 2019). Strains expressing GFP via vector pMP2444 (Table 1) were grown overnight and normalized at an OD_{600} of 0.5. Flow cell chambers in a μ-Slide VI (Ibidi) were inoculated with the cultures and incubated for 1 h at 24°C. Following this, a flow of 0.5 × LB medium was applied to the flow chambers using a peristaltic pump (Ismatec REGLO; Cole-Parmer) for 5 h. Biofilms were visualized using a FluoView 1000 confocal laser-scanning microscope (Olympus). *z*-Stacked images of the flow cell channels were processed by ImageJ and compared for the green fluorescence value using the RBG assessment plug-in (Schneider et al., 2012). Three replicates conducted in the study were statistically compared using Tukey's HSD on JMP statistical software.

4.9 | Intracellular c-di-GMP concentration measurement

Intracellular levels of c-di-GMP were determined via ultraperformance liquid chromatography/tandem mass spectrometry (UPLC-MS-MS) as previously described (Edmunds et al., 2013). Strains were grown in LB medium overnight at 28°C. Cells were collected and lysed (using 40% acetonitrile and 40% methanol vol/vol) at −20°C for 15 min. Samples were processed on a Quattro Premier XE instrument (Waters Corp.) against a gradient established with synthetic c-di-GMP (Axxora Life Sciences Inc.). Three replicates conducted in the study were statistically compared using Tukey's HSD on JMP statistical software.

4.10 | Ligand binding assays

Native and site-directed mutated versions of CsrD were extracted using *E. coli* BL21(DE3) transformed with the appropriate pET21-a (Novagen) vectors harbouring the target genes. Overnight cultures grown in LB medium at 37°C were subcultured until they reached an OD_{600} of 0.5. Induction of expression was conducted using 1 mM IPTG for 12 h at 25°C. Following this, cells were collected and lysed by sonification on ice for 60 s in Tris-buffered saline (TBS). HisPur Ni-NTA Resin (ThermoFisher Scientific) was used to purify the 6×His-tagged proteins under native conditions with TBS as per manufacturer's instructions and dialysed against TBS using the Slide-A-Lyzer MINI dialysis device (ThermoFisher Scientific) as per manufacturer's instructions. Initial protein concentration was determined using Pierce BCA Protein Assay Kit (ThermoFisher Scientific) as per manufacturer's instructions. Protein aliquots were stored in TBS at −20°C. Binding to c-di-GMP was assessed as in a previously described protocol, using the buffers and reagents mentioned by Chambers and Sauer (2017). Extracted proteins were treated with biotinylated c-di-GMP (Biolog Life Sciences) and/or unmarked c-di-GMP (Axxora Life Sciences) or GTP competitor (ThermoFisher Scientific), all at specific concentrations for 30 min at room temperature. Streptavidin magnetic beads (NEB) were used to pull down the bound c-di-GMP-protein complex. The eluted contents from the pull-down assay were blotted on a polyvinylidene difluoride (PVDF) membrane, followed by blocking with 1% (wt/vol) bovine serum albumen in TBS with 0.1% Tween 20 (vol/vol). Anti-His-horseradish peroxidase (HRP) (ThermoFisher Scientific) was used for antigen detection at a dilution of 1:10,000 as per manufacturer's instructions, visualized using the Clarity ECL substate (Bio-Rad) and imaged on a Chemidoc MP imager system

(Bio-Rad). ImageJ was used to process images to calculate binding K_D (dissociation constant) based on half maximal binding, as previously described (Chambers & Sauer, 2017).

4.11 | Relative gene expression using RT-qPCR

To measure *amsG*, *csrD*, and CsrB transcript levels, using RT-qPCR and northern blotting, overnight cultures grown at 28°C were induced with MBMA for 6 h at 28°C. RNA was extracted from the samples using the Direct-zol RNA kit (Zymo Research). A High-Capacity cDNA reverse transcription kit (ThermoFisher Scientific) was used to generate cDNA from the RNA extracts. Quantitative PCR was conducted using SYBR Green PCR master mix (Applied Biosystems). *recA* was used as an endogenous control. Relative fold change in expression levels were calculated based on the ΔC_t method (Rao et al., 2013). Three biological replicates were included in the experiments.

4.12 | Relative measurements of *CsrB* transcript abundance using RT-qPCR and northern blotting

To measure the relative levels of transcript degradation of *csrB* over time, strains grown overnight were transferred to MBMA for 6 h with IPTG as necessary (for *dgc* overexpresssion). At this stage, samples were taken from the strains and immediately processed to extract RNA. RNA (100 ng) was used to generate cDNA. Using *recA* as an endogenous control during RT-qPCR, the basal levels of *CsrB* (prior to beginning the transcript degradation experiment) were determined for the strains via the $\Delta\Delta C_t$ method (Rao et al., 2013). Strains were treated with rifampicin (500 μg/ml) and incubated for the appropriate experimental times before being immediately processed for total RNA extraction. RNA (100 ng) was used to generate cDNA. The C_t values (for *csrB*) for the control samples (0 min for each variant) were used to set the 100% relative mRNA threshold. Biotinylated RNA probes for northern blotting were generated by Sigma-Aldrich. The NorthernMax-Gly Kit, streptavidin-HRP-conjugated antibodies (ThermoFisher Scientific), and Clarity ECL substate (Bio-Rad) were used for blot processing and visualization via a ChemidocMP system (Bio-Rad). Statistical analysis included the comparison of the means via a Student's *t* test that compared the degradation metric for Ea1189Δ12 at each time point to all other strain variants at the respective time points. This analysis was conducted using JMP statistical software.

ACKNOWLEDGMENTS

This project was supported by funds from the Agriculture and Food Research Initiative Competitive Grants Program grant no. 2015-67013-23068 from the USDA National Institute of Food and Agriculture, and by Michigan State University AgBioResearch. R.R.K. is a Michigan State University Plant Science Initiative graduate fellow.

DATA AVAILABILITY STATEMENT

The data sets generated for this study are available on request to the corresponding author.

ORCID

George W. Sundin https://orcid.org/0000-0003-4078-8368

REFERENCES

Agbo, E.C., Duim, B., Majiwa, P.A., Buscher, P., Claassen, E. & Te Pas, M.F. (2003) Multiplex-endonuclease genotyping approach (MEGA): a tool for the fine-scale detection of unlinked polymorphic DNA markers. *Chromosoma*, 111, 518–524.

Amarasinghe, J.J., D'Hondt, R.E., Waters, C.M. & Mantis, N.J. (2013) Exposure of *Salmonella enterica* serovar Typhimurium to a protective monoclonal IgA triggers exopolysaccharide production via a diguanylate cyclase-dependent pathway. *Infection and Immunity*, 81, 653–664.

Ancona, V., Lee, J.H. & Zhao, Y. (2016) The RNA-binding protein CsrA plays a central role in positively regulating virulence factors in *Erwinia amylovora*. *Scientific Reports*, 6, 37195.

Andrade, M., Zhang, Y., Wang, W., Teper, D., Romeo, T. & Wang, N. (2021) Examination of the global regulon of CsrA in *Xanthomonas citri* subsp. *citri* using quantitative proteomics and other approaches. *Molecular Plant-Microbe Interactions*, 34, 1236–1249.

Barends, T.R., Hartmann, E., Griese, J.J., Beitlich, T., Kirienko, N.V., Ryjenkov, D.A. et al. (2009) Structure and mechanism of a bacterial light-regulated cyclic nucleotide phosphodiesterase. *Nature*, 459, 1015–1018.

Bernhard, F., Coplin, D.L. & Geider, K. (1993) A gene cluster for amylovoran synthesis in *Erwinia amylovora*: characterization and relationship to cps genes in *Erwinia stewartii*. *Molecular and General Genetics*, 239, 158–168.

Bobrov, A.G., Kirillina, O. & Perry, R.D. (2005) The phosphodiesterase activity of the HmsP EAL domain is required for negative regulation of biofilm formation in *Yersinia pestis*. *FEMS Microbiology Letters*, 247, 123–130.

Bugert, P. & Geider, K. (1995) Molecular analysis of the *ams* operon required for exopolysaccharide synthesis of *Erwinia amylovora*. *Molecular Microbiology*, 15, 917–933.

Carver, T., Harris, S.R., Berriman, M., Parkhill, J. & McQuillan, J.A. (2012) Artemis: an integrated platform for visualization and analysis of high-throughput sequence-based experimental data. *Bioinformatics*, 28, 464–469.

Chambers, J.R. & Sauer, K. (2017) Detection of cyclic di-GMP binding proteins utilizing a biotinylated cyclic di-GMP pull-down assay. *Methods in Molecular Biology*, 1657, 317–329.

Chatterjee, S., Killiny, N., Almeida, R.P. & Lindow, S.E. (2010) Role of cyclic di-GMP in *Xylella fastidiosa* biofilm formation, plant virulence, and insect transmission. *Molecular Plant-Microbe Interactions*, 23, 1356–1363.

Chin, K.H., Kuo, W.T., Yu, Y.J., Liao, Y.T., Yang, M.T. & Chou, S.H. (2012) Structural polymorphism of c-di-GMP bound to an EAL domain and in complex with a type II PilZ-domain protein. *Acta Crystallographica. Section D, Biological Crystallography*, 68, 1380–1392.

Chou, S.H. & Galperin, M.Y. (2016) Diversity of cyclic di-GMP-binding proteins and mechanisms. *Journal of Bacteriology*, 198, 32–46.

Christen, M., Kulasekara, H.D., Christen, B., Kulasekara, B.R., Hoffman, L.R. & Miller, S.I. (2010) Asymmetrical distribution of the second messenger c-di-GMP upon bacterial cell division. *Science*, 328, 1295–1297.

Datsenko, K.A. & Wanner, B.L. (2000) One-step inactivation of chromosomal genes in Escherichia coli K-12 using PCR products.

Proceedings of the National Academy of Sciences of the United States of America, 97, 6640–6645.

Dunn, A.K., Millikan, D.S., Adin, D.M., Bose, J.L. & Stabb, E.V. (2006) New rfp- and pES213-derived tools for analyzing symbiotic *Vibrio fischeri* reveal patterns of infection and lux expression in situ. *Applied and Environmental Microbiology*, 72, 802–810.

Duss, O., Michel, E., Yulikov, M., Schubert, M., Jeschke, G. & Allain, F.-H.-T. (2014) Structural basis of the non-coding RNA RsmZ acting as a protein sponge. *Nature*, 509, 588–592.

Ebel, W. & Trempy, J.E. (1999) *Escherichia coli* RcsA, a positive activator of colanic acid capsular polysaccharide synthesis, functions to activate its own expression. *Journal of Bacteriology*, 181, 577–584.

Edmunds, A.C., Castiblanco, L.F., Sundin, G.W. & Waters, C.M. (2013) Cyclic di-GMP modulates the disease progression of *Erwinia amylovora*. *Journal of Bacteriology*, 195, 2155–2165.

Erickson, D.L., Lew, C.S., Kartchner, B., Porter, N.T., McDaniel, S.W., Jones, N.M. et al. (2016) Lipopolysaccharide biosynthesis genes of *Yersinia pseudotuberculosis* promote resistance to antimicrobial chemokines. *PLoS One*, 11, e0157092.

Ferreiro, M.-D., Nogales, J., Farias, G.A., Olmedilla, A., Sanjuán, J. & Gallegos, M.T. (2018) Multiple CsrA proteins control key virulence traits in *Pseudomonas syringae* pv. *tomato* DC3000. *Molecular Plant-Microbe Interactions*, 31, 525–536.

Finn, R.D., Bateman, A., Clements, J., Coggill, P., Eberhardt, R.Y., Eddy, S.R. et al. (2014) Pfam: the protein families database. *Nucleic Acids Research*, 42, D222–D230.

Gervais, F.G., Phoenix, P. & Drapeau, G.R. (1992) The *rcsB* gene, a positive regulator of colanic acid biosynthesis in *Escherichia coli*, is also an activator of *ftsZ* expression. *Journal of Bacteriology*, 174, 3964–3971.

Gonzalez, G.M., Durica-Mitic, S., Hardwick, S.W., Moncrieffe, M.C., Resch, M., Neumann, P. et al. (2017) Structural insights into RapZ-mediated regulation of bacterial amino-sugar metabolism. *Nucleic Acids Research*, 45, 10845–10860.

Guzzo, C.R., Dunger, G., Salinas, R.K. & Farah, C.S. (2013) Structure of the PilZ–FimXEAL–c-di-GMP complex responsible for the regulation of bacterial type IV pilus biogenesis. *Journal of Molecular Biology*, 425, 2174–2197.

Hengge, R. (2021) High-specificity local and global c-di-GMP signaling. *Trends in Microbiology*, 29, 993–1003.

Hentzer, M., Teitzel, G.M., Balzer, G.J., Heydorn, A., Molin, S., Givskov, M. et al. (2001) Alginate overproduction affects *Pseudomonas aeruginosa* biofilm structure and function. *Journal of Bacteriology*, 183, 5395–5401.

Jenal, U., Reinders, A. & Lori, C. (2017) Cyclic di-GMP: second messenger extraordinaire. *Nature Reviews Microbiology*, 15, 271–284.

Johnson, M., Zaretskaya, I., Raytselis, Y., Merezhuk, Y., McGinnis, S. & Madden, T.L. (2008) NCBI BLAST: a better web interface. *Nucleic Acids Research*, 36, W5–W9.

Jonas, K., Edwards, A.N., Ahmad, I., Romeo, T., Romling, U. & Melefors, O. (2010) Complex regulatory network encompassing the Csr, c-di-GMP and motility systems of *Salmonella typhimurium*. *Environmental Microbiology*, 12, 524–540.

Kharadi, R.R., Castiblanco, L.F., Waters, C.M. & Sundin, G.W. (2019) Phosphodiesterase genes regulate amylovoran production, biofilm formation, and virulence in *Erwinia amylovora*. *Applied and Environmental Microbiology*, 85, e02233-18.

Kharadi, R.R., Selbmann, K. & Sundin, G.W. (2021) The cyclic di-GMP network is a global regulator of phase-transition and attachment-dependent host colonization in *Erwinia amylovora*. *bioRxiv*, 2021.02.01.429191. https://doi.org/10.1101/2021.02.01.429191

Kharadi, R.R. & Sundin, G.W. (2019) Physiological and microscopic characterization of cyclic-di-GMP-mediated autoaggregation in *Erwinia amylovora*. *Frontiers in Microbiology*, 10, 468.

Kharadi, R.R. & Sundin, G.W. (2020) Cyclic-di-GMP regulates autoaggregation through the putative peptidoglycan hydrolase, EagA, and regulates transcription of the *znuABC* zinc uptake gene cluster in *Erwinia amylovora*. *Frontiers in Microbiology*, 11, 605265.

Kharadi, R.R. & Sundin, G.W. (2021) Dissecting the process of xylem colonization through biofilm formation in *Erwinia amylovora*. *Journal of Plant Pathology*, 103(Suppl 1), S41–S49.

Koczan, J.M., McGrath, M.J., Zhao, Y. & Sundin, G.W. (2009) Contribution of *Erwinia amylovora* exopolysaccharides amylovoran and levan to biofilm formation: implications in pathogenicity. *Phytopathology*, 99, 1237–1244.

Kovach, M.E., Elzer, P.H., Hill, D.S., Robertson, G.T., Farris, M.A., Roop, R.M. et al. (1995) Four new derivatives of the broad-host-range cloning vector pBBR1MCS, carrying different antibiotic-resistance cassettes. *Gene*, 166, 175–176.

Kusmierek, M. & Dersch, P. (2018) Regulation of host–pathogen interactions via the post-transcriptional Csr/Rsm system. *Current Opinion in Microbiology*, 41, 58–67.

Lauro, F.M., Tran, K., Vezzi, A., Vitulo, N., Valle, G. & Bartlett, D.H. (2008) Large-scale transposon mutagenesis of *Photobacterium profundum* SS9 reveals new genetic loci important for growth at low temperature and high pressure. *Journal of Bacteriology*, 190, 1699–1709.

Ledeboer, N.A. & Jones, B.D. (2005) Exopolysaccharide sugars contribute to biofilm formation by *Salmonella enterica* serovar Typhimurium on HEp-2 cells and chicken intestinal epithelium. *Journal of Bacteriology*, 187, 3214–3226.

Lee, J.H., Ancona, V., Chatnaparat, T., Yang, H.-W. & Zhao, Y. (2019) The RNA-binding protein CsrA controls virulence in *Erwinia amylovora* by regulating RelA, RcsB, and FlhD at the posttranscriptional level. *Molecular Plant-Microbe Interactions*, 32, 1448–1459.

Lee, J.H., Ancona, V. & Zhao, Y. (2018) Lon protease modulates virulence traits in *Erwinia amylovora* by direct monitoring of major regulators and indirectly through the Rcs and Gac-Csr regulatory systems. *Molecular Plant Pathology*, 19, 827–840.

Leng, Y., Vakulskas, C.A., Zere, T.R., Pickering, B.S., Watnick, P.I., Babitzke, P. et al. (2016) Regulation of CsrB/C sRNA decay by EIIA(Glc) of the phosphoenolpyruvate: carbohydrate phosphotransferase system. *Molecular Microbiology*, 99, 627–639.

Liu, M.Y., Gui, G., Wei, B., Preston, J.F., Oakford, L., Yüksel, Ü. et al. (1997) The RNA molecule CsrB binds to the global regulatory protein CsrA and antagonizes its activity in *Escherichia coli*. *Journal of Biological Chemistry*, 272, 17502–17510.

Long, T., Tu, K.C., Wang, Y., Mehta, P., Ong, N.P., Bassler, B.L. et al. (2009) Quantifying the integration of quorum-sensing signals with single-cell resolution. *PLoS Biology*, 7, e68.

Lu, X.-H., An, S.-Q., Tang, D.-J., McCarthy, Y., Tang, J.-L., Dow, J.M. et al. (2012) RsmA regulates biofilm formation in *Xanthomonas campestris* through a regulatory network involving cyclic di-GMP and the Clp transcription factor. *PLoS One*, 7, e52646.

Miller, W.G., Leveau, J.H. & Lindow, S.E. (2000) Improved *gfp* and *inaZ* broad-host-range promoter-probe vectors. *Molecular Plant-Microbe Interactions*, 13, 1243–1250.

Minasov, G., Padavattan, S., Shuvalova, L., Brunzelle, J.S., Miller, D.J., Baslé, A. et al. (2009) Crystal structures of YkuI and its complex with second messenger cyclic di-GMP suggest catalytic mechanism of phosphodiester bond cleavage by EAL domains. *Journal of Biological Chemistry*, 284, 13174–13184.

Nadell, C.D. & Bassler, B.L. (2011) A fitness trade-off between local competition and dispersal in Vibrio cholerae biofilms. *Proceedings of the National Academy of Sciences of the United States of America*, 108, 14181–14185.

Navarro, M.V., De, N., Bae, N., Wang, Q. & Sondermann, H. (2009) Structural analysis of the GGDEF-EAL domain-containing c-di-GMP receptor FimX. *Structure*, 17, 1104–1116.

Navarro, M.V., Newell, P.D., Krasteva, P.V., Chatterjee, D., Madden, D.R., O'Toole, G.A. et al. (2011) Structural basis for c-di-GMP-mediated inside-out signaling controlling periplasmic proteolysis. *PLoS Biology*, 9, e1000588.

Perez-Mendoza, D., Aragon, I.M., Prada-Ramirez, H.A., Romero-Jimenez, L., Ramos, C., Gallegos, M.-T. et al. (2014) Responses to elevated c-di-GMP levels in mutualistic and pathogenic plant-interacting bacteria. *PLoS One*, 9, e91645.

Petanidou, T. (2005) Sugars in Mediterranean floral nectars: an ecological and evolutionary approach. *Journal of Chemical Ecology*, 31, 1065–1088.

Pickering, B.S., Smith, D.R. & Watnick, P.I. (2012) Glucose-specific enzyme IIA has unique binding partners in the *Vibrio cholerae* biofilm. *mBio*, 3, e00228-12.

Rao, X., Huang, X., Zhou, Z. & Lin, X. (2013) An improvement of the $2^{(-\Delta\Delta Ct)}$ method for quantitative real-time polymerase chain reaction data analysis. *Biostatistics, Bioinformatics and Biomathematics*, 3, 71–85.

Riley, M., Abe, T., Arnaud, M.B., Berlyn, M.K., Blattner, F.R., Chaudhuri, R.R. et al. (2006) *Escherichia coli* K-12: a cooperatively developed annotation snapshot–2005. *Nucleic Acids Research*, 34, 1–9.

Romling, U., Galperin, M.Y. & Gomelsky, M. (2013) Cyclic di-GMP: the first 25 years of a universal bacterial second messenger. *Microbiology and Molecular Biology Reviews*, 77, 1–52.

Sambrook, J. & Russell, D.W. (2001) *Molecular cloning: a laboratory manual*. New York: Cold Spring Harbor Laboratory Press.

Schmidt, H.A., Strimmer, K., Vingron, M. & von Haeseler, A. (2002) TREE-PUZZLE: maximum likelihood phylogenetic analysis using quartets and parallel computing. *Bioinformatics*, 18, 502–504.

Schneider, C.A., Rasband, W.S. & Eliceiri, K.W. (2012) NIH Image to ImageJ: 25 years of image analysis. *Nature Methods*, 9, 671–675.

Sievers, F. & Higgins, D.G. (2014) Clustal omega. *Current Protocols in Bioinformatics*. 48, 1–16.

Simon, R., Quandt, J. & Klipp, W. (1989) New derivatives of transposon Tn*5* suitable for mobilization of replicons, generation of operon fusions and induction of genes in gram-negative bacteria. *Gene*, 80, 161–169.

Smits, T., Duffy, B., Sundin, G., Zhao, Y. & Rezzonico, F. (2017) *Erwinia amylovora* in the genomics era: from genomes to pathogen virulence, regulation, and disease control strategies. *Journal of Plant Pathology*, 99, 7–23.

Stuurman, N., Pacios Bras, C., Schlaman, H.R., Wijfjes, A.H., Bloemberg, G. & Spaink, H.P. (2000) Use of green fluorescent protein color variants expressed on stable broad-host-range vectors to visualize rhizobia interacting with plants. *Molecular Plant-Microbe Interactions*, 13, 1163–1169.

Suzuki, K., Babitzke, P., Kushner, S.R. & Romeo, T. (2006) Identification of a novel regulatory protein (CsrD) that targets the global regulatory RNAs CsrB and CsrC for degradation by RNase E. *Genes & Development*, 20, 2605–2617.

Suzuki, K., Wang, X., Weilbacher, T., Pernestig, A.-K., Melefors, O., Georgellis, D. et al. (2002) Regulatory circuitry of the CsrA/CsrB and BarA/UvrY systems of *Escherichia coli*. *Journal of Bacteriology*, 184, 5130–5140.

Tchigvintsev, A., Xu, X., Singer, A., Chang, C., Brown, G., Proudfoot, M. et al. (2010) Structural insight into the mechanism of c-di-GMP hydrolysis by EAL domain phosphodiesterases. *Journal of Molecular Biology*, 402, 524–538.

Vakulskas, C.A., Leng, Y., Abe, H., Amaki, T., Okayama, A., Babitzke, P. et al. (2016) Antagonistic control of the turnover pathway for the global regulatory sRNA CsrB by the CsrA and CsrD proteins. *Nucleic Acids Research*, 44, 7896–7910.

Wang, D., Korban, S.S. & Zhao, Y. (2009) The Rcs phosphorelay system is essential for pathogenicity in *Erwinia amylovora*. *Molecular Plant Pathology*, 10, 277–290.

Wang, D., Qi, M., Calla, B., Korban, S.S., Clough, S.J., Cock, P.J. et al. (2012) Genome-wide identification of genes regulated by the Rcs phosphorelay system in *Erwinia amylovora*. *Molecular Plant-Microbe Interactions*, 25, 6–17.

Waters, C.M., Lu, W., Rabinowitz, J.D. & Bassler, B.L. (2008) Quorum sensing controls biofilm formation in *Vibrio cholerae* through modulation of cyclic di-GMP levels and repression of vpsT. *Journal of Bacteriology*, 190, 2527–2536.

Yang, F., Qian, S., Tian, F., Chen, H., Hutchins, W., Yang, C.H. et al. (2016) The GGDEF-domain protein GdpX1 attenuates motility, exopolysaccharide production and virulence in *Xanthomonas oryzae* pv. *oryzae*. *Journal of Applied Microbiology*, 120, 1646–1657.

Yang, F., Tian, F., Li, X., Fan, S., Chen, H., Wu, M. et al. (2014) The degenerate EAL-GGDEF domain protein Filp functions as a cyclic di-GMP receptor and specifically interacts with the PilZ-domain protein PXO_02715 to regulate virulence in *Xanthomonas oryzae* pv. *oryzae*. *Molecular Plant-Microbe Interactions*, 27, 578–589.

Yu, M., Singh, J., Khan, A., Sundin, G.W. & Zhao, Y. (2020) Complete genome sequence of the fire blight pathogen strain *Erwinia amylovora* Ea1189. *Molecular Plant-Microbe Interactions*, 33, 1277–1279.

Yuan, X., Khokhani, D., Wu, X., Yang, F., Biener, G., Koestler, B.J. et al. (2015) Cross-talk between a regulatory small RNA, cyclic-di-GMP signalling and flagellar regulator FlhDC for virulence and bacterial behaviours. *Environmental Microbiology*, 17, 4745–4763.

Zhang, X.-S., García-Contreras, R. & Wood, T.K. (2008) Escherichia coli transcription factor YncC (McbR) regulates colanic acid and biofilm formation by repressing expression of periplasmic protein YbiM (McbA). *The ISME Journal*, 2, 615–631.

Zhao, Y., Sundin, G.W. & Wang, D. (2009) Construction and analysis of pathogenicity island deletion mutants of *Erwinia amylovora*. *Canadian Journal of Microbiology*, 55, 457–464.

SUPPORTING INFORMATION

Additional supporting information may be found in the online version of the article at the publisher's website.

How to cite this article: Kharadi, R.R. & Sundin, G.W. (2022) CsrD regulates amylovoran biosynthesis and virulence in *Erwinia amylovora* in a novel cyclic-di-GMP dependent manner. *Molecular Plant Pathology*, 23, 1154–1169. https://doi.org/10.1111/mpp.13217